JAST, Vol. 10, No. 2, pp. 17- 23

JAST
Journal of Aerospace Science and Technology

Real Time Calibration of Strap-down Three-Axis-Magnetometer for Attitude Estimation

M. Kiani[1]* and S. H. Pourtakdoust[2]

1, 2. Department of Aerospace Engineering, Sharif University of Technology

*Postal Code:1458889694, Tehran, IRAN

m_kiani@ae.sharif.ir

Three-axis-magnetometers (TAMs) are widely utilized as a key component of attitude determination subsystems and as such are considered the corner stone of navigation for low Earth orbiting (LEO) space systems. Precise geomagnetic-based navigation demands accurate calibration of the magnetometers. In this regard, a complete online calibration process of TAM is developed in the current research that considers the combined effects of environmental and instrumental errors including biases, non-orthogonally parameters ,and the scale factors, without the need for clean room facilities. The sensor characteristics are estimated utilizing Kalman filter for a micro electro-mechanical sensor(MEMS)-based TAM standing on the experimental measured outputs in a noisy laboratory environment. Moreover, the stochastic TAM behavior is identified using the method of Allan variance analysis (AVA) through a six-hour static test. Subsequently, the nonlinear/non-Gaussian problem of attitude estimation, using a set of calibrated strap-down magnetometers is addressed utilizing the unscented particle filter (UPF), developed for the removal of colored-noise. Comparison of the estimated attitude, represented by quaternion parameters, with the true orientations demonstrates an acceptable level of accuracy of the developed calibration technique for small LEO space systems. Analysis of the root mean square error of the estimated attitude illustrates an accuracy of less than one degree for all axes. This is an ideal result, given the fact that MEMS-based magnetometers have been utilized.

Keywords: Magnetometer calibration, Allan Variance, Kalman filter, Attitude estimation, Unscented particle filter

Nomenclature

ϕ	Rotation angle
$\mathbf{q}$	Vector of quaternion parameters
$\boldsymbol{\omega}^{BN}$	Angular velocity of the body frame respect to the navigation frame
$\mathbf{b}^{hi}$	Hard iron bias vector
$\mathbf{b}^{so}$	Soft iron bias vector
$\mathbf{S}$	Vector of scale factors
$\mathbf{M}$	Misalignment matrix
$\mathbf{H}$	Geomagnetic field vector
T^{BN}	Coordinate transformation matrix of body frame with respect to navigation frame
$\mathbf{P}$	Estimation error covariance matrix
$\mathbf{x}$	State vector
$\mathbf{w}$	Process noise vector
$\mathbf{z}$	Measurement vector
$\mathbf{v}$	Measurement noise vector
$\boldsymbol{\psi}$	Transition matrix of the colored noise
ζ	Zero-mean Gaussian white noise
$\mathbf{Q}$	Covariance matrix of the process noise
$\mathbf{R}$	Covariance matrix of the measurement noise
$E(\mathbf{x})$	Expectation operator of $\mathbf{x}$
δ_{kl}	Kronecker delta function

Introduction

Three-axis magnetometer (TAM) is an essential component of many navigation packs for LEO satellites. TAM is utilized in vast areas of aerial-, space-, and earth-navigation robots as well as human body kinematics estimation. Special features of TAM

1. Professor (Corresponding Author)
2. M. Sc.

such as low cost, small size, lightweight, reliability and low power requirements are some of the key reasons for its widespread application (Wu et al., 2011). TAMs can provide suitable estimations of space system attitude and position via measuring the geomagnetic field along the body axes. There for e, TAM has been selected as the most popular attitude sensor in cube satellites. However, due to a number of limitations and inadequacies in manufacturing, installation and material as well as the environmental influences, their output is usually contaminated with different errors. In general, bias, scale factor and non-orthogonally parameters are the most important error parameters for three-dimensional (3D) field sensors like TAMs. Obviously, such erroneous measurements cannot provide accurate estimations of the vehicle's attitude or position, hence, sensor calibration is an essential requirement for the purpose of precise navigation.

Magnetometer calibration is not a new topic and has been addressed in numerous researches before. There is a wide variety of mathematical methods for sensor calibration, but they can all be classified into two main groups of batch estimation and recursive estimation. Batch estimators need a batch of measured data to provide an estimation of the parameter and/or state vectors, while the recursive filters estimate the parameters or states recursively upon the progressive receipt of the measurement data. The method of least square error is the most widespread scheme utilized for offline calibration of TAMs. Zhang et al. (2014) have utilized the homogenous least square error method to estimate the error parameters and orientation. Furthermore, Zhang et al. (2009) have transformed the TAM calibration problem to an ellipsoid-fitting issue and adopted the direct least square scheme for its

solution. Wu et al. (2011) have transformed the nonlinear problem of attitude-independent TAM calibration to a parameter optimization problem using particle swarm optimization (PSO). It is claimed that PSO-based calibration provides better results as compared with the so-called two-step method (Gebre-Egziabher &Elkaim, 2011).

Since most of the dominant sources of sensor errors are usually time varying, offline calibration cannot compensate their effects completely. In this regard, Crassidis et al. (2005) have used nonlinear filters of the extended Kalman filter (EKF) and the unscented Kalman filter (UKF) for the sequential calibration of the TAM in real time. It is shown that the accuracy level of both filters are the same, but UKF is more robust against large initial errors. Soken and Hajiev (2011) have also utilized a reconfigurable UKF to estimate bias and scale factor parameters as part of an attitude estimation problem. Beravs et al. (2014) have utilized a precise 3D Helmholtz coil for the magnetometer calibration using UKF. Their proposed method repeatedly uses the covariance matrix decomposition for the estimation of the maximal sensitivity axis to assess the next best orientation of the coil magnetic field. Vasconcelos et al. (2011) have formulated a maximum likelihood estimator to find the optimal calibration parameters iteratively. Initial conditions for the iterative algorithm are also obtained using a suboptimal batch least square computation.

In the present study, recursive calibration of TAM in a noisy test facility is considered,where the error parameters are modeled as a random walk process. Kalman filter is the optimal choicefor the parameter estimation of such linear systems. However, Investigation of the stochastic behavior of the tested Honeywell TAM disclosed non-Gaussian/non-white behavior of the measured signals. Therefore, a colored-noise unscented particle filter (UPF) was further developed to cope with the nonlinear problem of attitude estimation using the calibrated TAM.

The remaining sections of this paper are organized as follows. First, the attitude kinematics is described. Next, the magnetometer errors and the pertinent modelings are introduced. Subsequently, the calibration algorithm is elaborated on, followed by experimental results obtained from the laboratory tests of a Honeywell HMC5883L magnetometer. The final part of the paper summarizes the results and addresses some future prospects for further research.

Attitude Kinematics

Attitude kinematics describes how the orientation of a vehicle changes under the influence of its angular velocity. There are various methods to represent the vehicle's attitude such as the Euler angles, quaternion parameters, Gibbs vector, direction cosine matrix, etc. (Shuster, 1993). The method of quaternion parameters is the most desired and widely used means to characterize the attitude, due to its linear propagation equation and its non-singular feature for any arbitrary rotation angle. The constraint of unit norm is the only disadvantage of the quaternion parameters which needs to be met in every estimation problem.
The quaternion parameters can propagate in time as follows (Zipfel, 2000),

$$\dot{\mathbf{q}} = \frac{1}{2}\Omega(\omega^{BN})\mathbf{q} \tag{1}$$

Where

$\mathbf{q} = [q_1 \quad q_2 \quad q_3 \quad q_4]^T = [n_1 \sin(\phi/2) \quad n_2 \sin(\phi/2) \quad n_3 \sin(\phi/2) \quad \cos(\phi/2)]^T$
, and

$$\Omega(\boldsymbol{\omega}^{BN}) = \begin{bmatrix} K\varepsilon & \omega_z & -\omega_y & \omega_x \\ -\omega_z & K\varepsilon & \omega_x & \omega_y \\ \omega_y & -\omega_x & K\varepsilon & \omega_z \\ -\omega_x & -\omega_y & -\omega_z & K\varepsilon \end{bmatrix} \tag{2}$$

In which $\mathbf{n} = [n_1 \quad n_2 \quad n_3]^T$ is the axis of rotation and ϕ is the angle of rotation. q_4 is also considered the scalar part of the quaternion, $\mathbf{q}$, $\varepsilon = 1 - \mathbf{q}^T\mathbf{q}$, and $\boldsymbol{\omega}^{BN} = [\omega_x \quad \omega_y \quad \omega_z]^T$ as well. The diagonal elements of $\Omega(\boldsymbol{\omega}^{BN})$ are especially written as shown to guarantee the unit norm requirement even in the presence of rounding errors and K is a constant to be selected so that $K\Delta t \le 1$ (Zipfel, 2000).

Magnetometer Error Modeling

Magnetometer output is corrupted by different errors. These errors include biases (offsets), scale factors, non-orthogonally parameters and setup errors that can be categorized into two main groups of environmental and instrumental errors. Interfering magnetic fields, known as environmental errors, consist of hard iron and soft iron errors which are dependent on the data gathering or sampling location. Although changing the test environment reduces the environmental errors, finding a magnetically isolated clean room is not always feasible in practice.

Hard iron perturbations that stem from permanent magnets or slow time-varying fieldsresult in a fixed magnetic deviation and thus are modeled as constant bias for the test area, $\mathbf{b}^{hi} = [b_x^{hi} \quad b_y^{hi} \quad b_z^{hi}]^T$. In contrast, the interaction of ferromagnetic material with an external field induces magnetism that changes both the direction and strength of the sensed field. This type of error called soft iron effect depends on the data sampling location and the instrumentations surrounding the TAM. Soft iron effect is modeled via a symmetric matrix $\mathbf{C}^{si}$. In addition to the environmental influences, instrumentation errors such as biases ($\mathbf{b}^{so} = [b_x \quad b_y \quad b_z]^T$), scale factors ($\mathbf{S} = diag(S_x, S_y, S_z)$), and misalignments ($\mathbf{M}$) are the other group of errors. Consequently, a comprehensive measurement model for the TAM can be remarked as,

$$\mathbf{B}_m = \mathbf{SM}(\mathbf{C}^{si}[\mathbf{H}]^B + \mathbf{b}^{hi}) + \mathbf{b}^{so} + \mathbf{v} \tag{3}$$

Where $[\mathbf{H}]^B$ is the true geomagnetic field vector expressed in the body coordinate system, and $\mathbf{v}$ is the measurement noise. Furthermore, the above formulation can be simply written as:

$$\mathbf{B}_m = \mathbf{C}[\mathbf{H}]^B + \mathbf{b} + \mathbf{v} \tag{4}$$

Where $\mathbf{C} = \mathbf{SMC}^{si}$ and $\mathbf{b} = \mathbf{SMb}^{hi} + \mathbf{b}^{so}$. Therefore, the problem of TAM calibration is reduced to determination of matrix $\mathbf{C}$ and vector $\mathbf{b}$ which include combined effects of error sources.

The geomagnetic field expressed in body coordinate system, $[\mathbf{H}]^B$, is provided by the available information in the navigation coordinate system as below:

$$[\mathbf{H}]^B = T^{BN}[\mathbf{H}]^N \tag{5}$$

where $[\mathbf{H}]^N$ is the geomagnetic field vector expressed in the navigation coordinate system; and calculated using the international geomagnetic reference field (IGRF) model (Finlay, Maus et al., 2010). Moreover, T^{BN} is the transformation matrix of the body coordinate system with respect to the navigation coordinate system defined as a function of the quaternion parameters as,

$$T^{BN} = \begin{bmatrix} q_1^2 - q_2^2 - q_3^2 + q_4^2 & 2(q_1q_2 + q_3q_4) & 2(q_1q_3 - q_2q_4) \\ 2(q_1q_2 - q_3q_4) & -q_1^2 + q_2^2 - q_3^2 + q_4^2 & 2(q_2q_3 + q_1q_4) \\ 2(q_1q_3 + q_2q_4) & 2(q_2q_3 - q_1q_4) & -q_1^2 - q_2^2 + q_3^2 + q_4^2 \end{bmatrix} \tag{6}$$

Attitude Determination and Magnetometer Parameter Estimation

The measurement model described in the previous section is a linear function of the TAM parameters, while it is a nonlinear function of the vehicle attitude characterized by the quaternion parameters. The combined error parameters of TAM are modeled as random walk process, i.e.

$$\dot{\theta} = w \tag{7}$$

Where $\theta = [\mathbf{b} \quad C_{ij}]^T$, $i, j = 1..3$. w is the process noise usually considered zero mean and white.

As it is shown in the next section, statistical analysis of the measurement signals illustrates non-Gaussian form of the probability distribution function (pdf). Therefore, Gaussian approximation algorithms such as EKF or UKF cannot estimate the attitude of the vehiclein a correct and precise way. Nevertheless, particle filter (PF) has been presented as a good remedy to deal with non-Gaussian pdfs, butit unfortunately ignores the most recent evidence and as a result the state estimation performance degrades (Van der Merwe et al., 2000). In this respect, PF is hybridized with another filter like EKF or UKF to improve theestimationefficiency. As UKF is more efficient than EKF for state estimation of the nonlinear dynamic systems, unscented particle filter (UPF) is adopted in the present study to cope with the current nonlinear/non-Gaussian problem of attitude estimation (Van der Merwe, et al., 2000).

Since the dynamics and measurement equations are linear with respect to TAM error parameters, a linear Kalman filter (KF), known as an optimal

estimator for Gaussian/Non-Gaussian linear systems is used to estimate the linear part, while the nonlinear part is handled with UPF.

An other issue about the considered attitude determination (AD) and calibration model is that the measurement noise has a variable power spectral density (PSD) function that denotes the measurement noise and is colored, as opposed to the white.

Colored noise is usually represented by a first order Markov process. To handle the time-correlated noise in the well-known filtering structure of Kalman, Bryson and Henrikson (1968) developed two strategies. The first approach augments the time-correlated measurement error into the state vector. This alternative is simple to implement, but increases the state space dimension and subsequently raises the run time. This method is also prone to divergence due to the singularity of the updated error covariance matrix. The second approach that is more complex is based on time differencing. Petovello et al. (2009) modified the measurement difference method to compensate 1-epoch latency in the second method of Bryson's, but his method diverges if the state transition matrix is ill conditioned. As a result, time differencing approach is more likely to converge. Recently, Wang et al. (2012) have proposed two new algorithms to deal with numerical problem of state augmentation alternative by perturbing the estimation error covariance matrix ($\mathbf{P}$) and regularizing the gain matrix. However, as the results show, perturbing $\mathbf{P}$ provides a reasonable solution, if and only if the perturbation amount is chosen appropriately, while there is no assured strategy to tune it. On the other hand, the other remedy is based on approximating the gain matrix according to Tikhonov regularization criterion. This approach needs a time-consuming iterative optimization to control the approximation error. Wang et al. (2012) have indicated that four mentioned algorithms have almost the same accuracy, but the operating time of the perturbed-$\mathbf{P}$ algorithm is the lowest. However, to avoid the ad-hoc strategy for tuning the required perturbation in perturbed-$\mathbf{P}$ algorithm, a time difference method is generalized in the current work for nonlinear state estimation in the presence of colored measurement noise.

The general discrete form of the attitude determination problem is as follows,

$$\mathbf{x}_k = \mathbf{f}_{k-1}(\mathbf{x}_{k-1}) + \mathbf{G}_{k-1}\mathbf{w}_{k-1} \tag{8}$$

$$\mathbf{z}_k = \mathbf{h}_k(\mathbf{x}_k) + \mathbf{v}_k \tag{9}$$

$$\mathbf{v}_k = \boldsymbol{\psi}_{k-1}\mathbf{v}_{k-1} + \zeta_{k-1}\,. \tag{10}$$

Where

$$\begin{aligned} &E(\mathbf{w}_k) = E(\zeta_k) = 0 \\ &E(\mathbf{w}_k\mathbf{w}_l^T) = \mathbf{Q}_k\delta_{kl}, \quad E(\zeta_k\zeta_l^T) = \mathbf{R}_k\delta_{kl}, \quad E(\mathbf{w}_k\zeta_l^T) = 0 \end{aligned} \tag{11}$$

$\mathbf{x}_k$ is the state vector at time t_k; $\mathbf{w}_k$ is the process noise vector, $\mathbf{z}_k$ is the measurement vector, $\mathbf{v}_k$ is the measurement noise and $\boldsymbol{\psi}_k$ is the transition matrix of the colored noise. ζ_k is the zero-mean Gaussian white noise, $E(\mathbf{x})$ is the expectation of $\mathbf{x}$, δ_{kl} is the Kronecker delta function, and $\mathbf{Q}_k$ and $\mathbf{R}_k$ are the covariance matrices of $\mathbf{w}_k$ and ζ_k, respectively. In order to make the measurement noise white, it is sufficient to introduce an auxiliary vector as below,

$$\begin{aligned} \mathbf{z}_k^* &= \mathbf{z}_k - \boldsymbol{\psi}_{k-1}\mathbf{z}_{k-1} \\ &= (\mathbf{h}_k - \boldsymbol{\psi}_{k-1}\mathbf{h}_{k-1}) + \zeta_{k-1} \\ &= \mathbf{h}_k^* + \zeta_{k-1} \end{aligned} \tag{12}$$

Regarding this vector as the new measurement vector, in addition to discrete dynamic system in eq. (8), an appropriate state space is now defined to utilize the Kalman filter for TAM calibration and the UPF for attitude determination.

Experiments and Analysis

To assess the performance of the proposed attitude determination and the calibration algorithm, laboratory experiments are conducted on a Honeywell HMC5883L 3D magnetometer in the noisy laboratory environment. HMC5883L is utilized in different areas such as auto navigation systems, mobile phones, consumer electronics, and personal navigation devices.

Allan variance (AV) is a simple method to model the sensor noise components (Hou, 2004). AV analysis is applied to the recorded TAM measurements in a static test lasting6 hours and sampled at the frequency of 10 Hz. Figure 1 shows the corresponding Allan deviation for the three axes of HMC5883L TAM. This figure clearly indicates that the bias instability and drift rate ramp are the dominant noise components along all the three axes. Figure 2 depicts the logarithmic diagram of noise power spectral density (PSD) versus the frequency. This figure obviously illustrates that x, y, and z noise components are pink and brown with powers of 1.9, 1.2 and 2.3, respectively. Probability density functions (pdfs) of the tested HMC5883L components are depicted in Figure 3. It is observed that all three axes have bimodal distributions, as opposed to Gaussian.

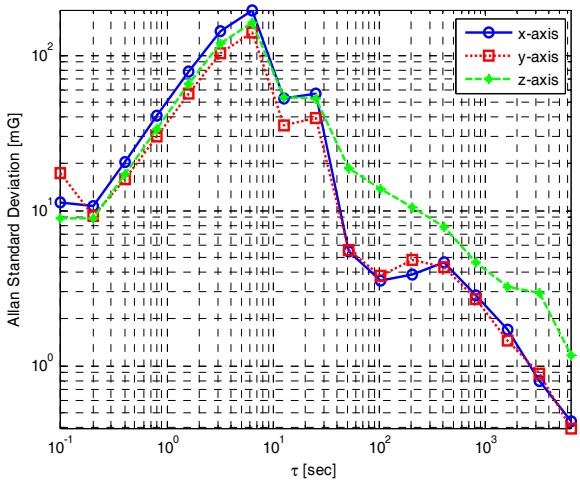

Figure 1. Honeywell HMC5883L Allan variance results

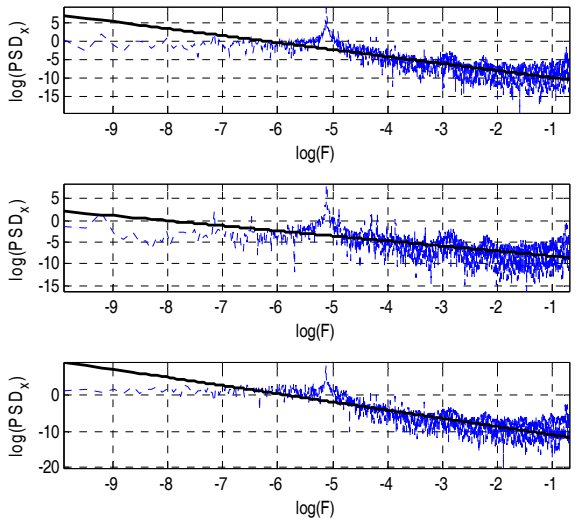

Figure 2. Power spectral density of TAM components

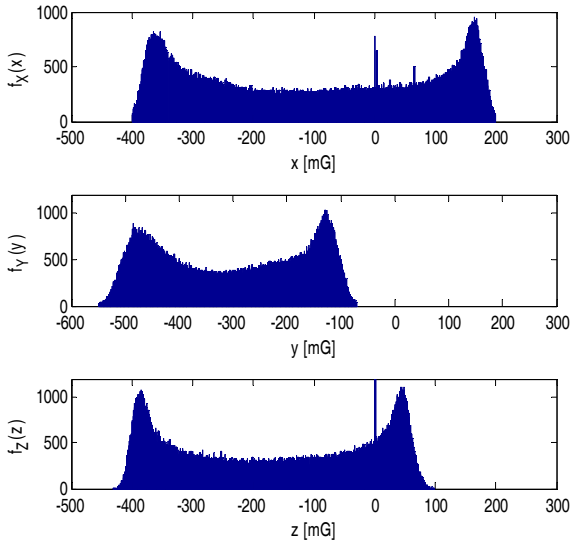

Figure 3. Probability density function (PDF) of TAM components

Complete calibration of a 3D field sensor such as TAM utilizing recursive estimation algorithms requiresan angular velocity to meet the persistency of excitation condition (Pittelkau, 2001). To this aim, the HMC5883L is set on a rotating turntable with an approximate angular velocity of $\boldsymbol{\omega}^{BN} = [0 \;\; 0 \;\; 20]^T$ (deg/ sec) in a laboratory at Sharif University of technology (SUT). Time history of the estimated combined error parameters including scale factors, non-orthogonally parameters and soft iron effect are depicted in Figure 4 and Figure 5. Time history of the combined bias including hard iron effect and sensor offset is also presented in Figure 6.Time history of measurement residual (innovation) is also shown in Figure 7. The zero-mean innovation depicted in this figure undoubtedly verifies the performance of the implemented estimation algorithm. Finally, Figure 8 depicts the time history of the innovations as well as their pertinent $\pm 2\sigma$ bounds. Note that the residual measurement has remained in its $\pm 2\sigma$ bounds. This observation is another proof to confirm the validity of the estimation process and reliability of the estimated states.

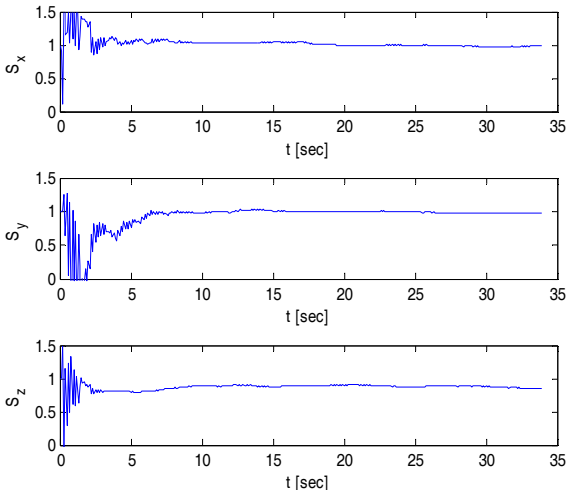

Figure 4. Time history of estimated combined scale factors

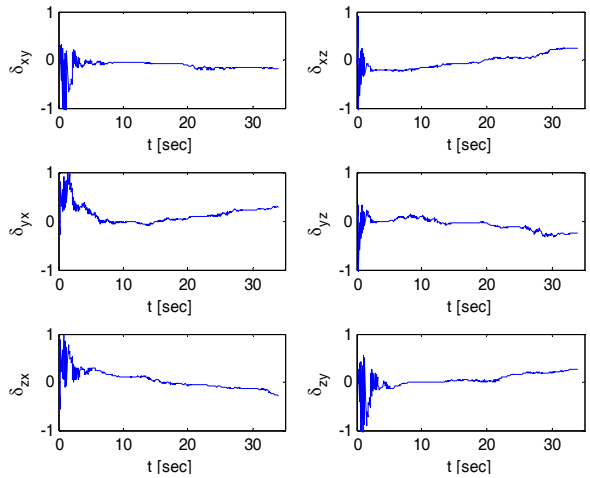

Figure 5. Time history of estimated combined non-orthogonally parameters

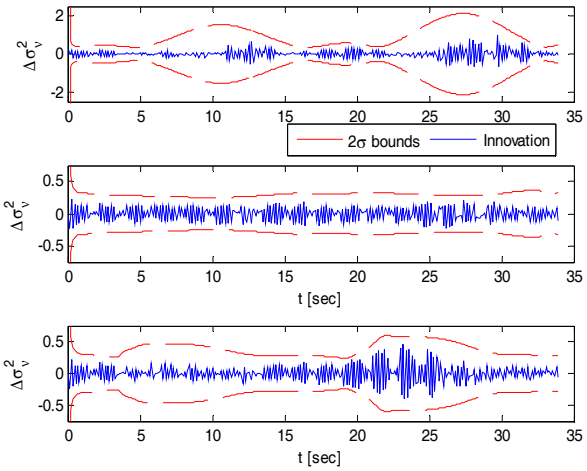

Figure 6. Innovation and pertinent $\pm 2\sigma$ bounds

As emphasized earlier, attitude determination will be performed subsequent to the TAM calibration to demonstrate the effectiveness of the proposed procedure. In this regard, Figure 9 shows the time history of the estimated and true quaternion parameters. It is worth mentioning that true attitude is accessible due to the experimental set up and the attitude kinematics. Figure 10 depicts the estimated and true attitudes in terms of the Euler angles. In addition, this figure compares the performance of the proposed UPF with EKF for the current AD problem. Since the current AD problem is non-Gaussian, colored-noise EKF cannot fulfill the estimation process and diverges, as indicated before. Calculation of the root mean square error (RMSE) of estimated Euler angles proves that estimation accuracy is less than 0.6 *deg* in roll angle (ϕ), 0.8 *deg* in pitch angle (θ), and 1 *deg* in yaw angle (ψ). The achieved accuracy is acceptable and suitable for most space missions.

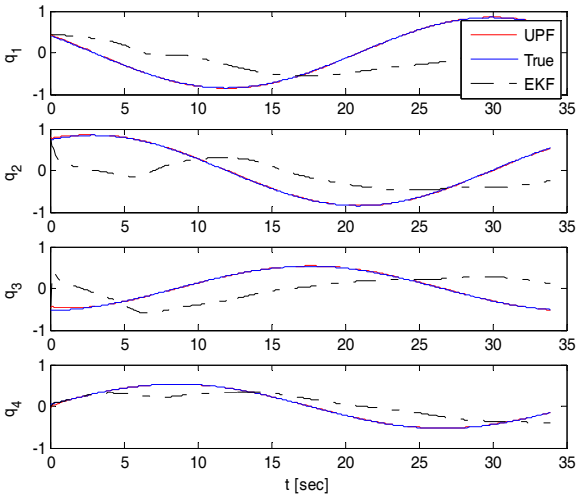

Figure 7. Time history of estimated and true quaternion parameters

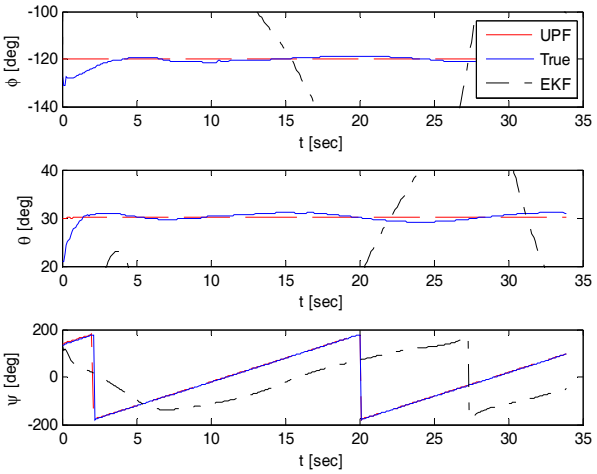

Figure 8. Time history of estimated and true Euler angles

Conclusion

Recursive calibration procedure of a three-axis magnetometer (TAM) is presented for attitude determination (AD) problem. Calibration module consists of real time estimation of error parameters including bias, scale factor and non-orthogonally parameters. Calibration parameters are modeled as random walk process and estimated via Kalman filter.
Statistical analysis over the sampled data for a micro electro-mechanical sensor (MEMS)-based TAM, Honeywell HMC5883L, using the Allan variance method has introduced the main noise components as well as the nature of the measurement noise color. In addition, considering the resulting bimodal probability density function of the measurement signals, a colored-noise unscented particle filter (UPF) is developed for the nonlinear attitude determination problem.

The laboratory experiments on a Honeywell HMC5883L demonstrate the potential applicability and acceptable performance of the colored-noise UPF for AD and TAM calibration. Moreover, comparison of the results emanating the proposed colored-noise UPF with those of the extended Kalman filter (EKF) provesa superior performance of the implemented UPF for AD application. Analysis of the root mean square error of the estimated attitude demonstrates that the vehicle attitude is determined with an accuracy of less than one degree for all axes. This is an ideal result; given the fact that MEMS-based magnetometer has been utilized.
Although, the experiments have been performed under approximately fixed temperature condition, the temperature dependency of the MEMS magnetometer such as the utilized HMC5883L is of importance for real world application. This issue will be further investigated by the authors to facilitate future integrated application of the calibrated TAM sensor for attitude estimation.

References

1. Beravs, T., Begus, S., Podobnik, J. and Munih, M., "Magnetometer Calibration Using Kalman Filter Covariance Matrix for Online Estimation of Magnetic Field Orientation," *IEEE Transactions on Instrumentation and Measurement*, Vol. 63, No. 8, 2014, pp. 2013-2020.
2. Bryson, A. E. Jr. and Henrikson, L.J., 1968, Estimation Using Sampled Data Containing Sequentially Correlated Noise, *Journal of Spacecraft and Rockets*, Vol. 5, pp. 662-665.
3. Crassidis, J. L., Lai K. L., Harman, R. R., "Real-Time Attitude-Independent Three-Axis Magnetometer Calibration," *Journal of Guidance, Control and Dynamics*, Vol. 28, No.1, 2005, pp. 115-120.
4. Finlay, C. C., Maus S., Beggan C. D., International Geomagnetic Reference Field: The Eleventh Generation, *Geophysical Journal international*, Vol. 183, 2010, pp. 1216-1230.
5. Gebre-Egziabher, D., Elkaim, G. H., Powell, J. D. and Parkinson, B. W., "A Nonlinear, Two-Step Algorithm for Calibration Solid-State Strap Down Magnetometers," *Proceeding of 8th International Conference on Navigation Systems, St. Petersburg,* Russia, 2001, pp. 200-299.
6. Hou, H., Modeling Inertial Sensors Errors using Allan Variance, [M. Sc. Thesis], Department of Geomatics Engineering, University of Calgary, 2004.
7. Petovello, M. G., O'Keefe, K., Lachapelle, G. and Cannon M. E., "Consideration of Time-Correlated Errors in a Kalman Filter Applicable to GNSS," *Journal Geodesy*, 2009, Vol. 83, pp. 51-59.
8. Pittelkau, M. E., "Kalman Filtering for Spacecraft System Alignment Calibration," *Journal of Guidance, Control, and Dynamics,* Vol. 24, No.6, 2001, 1187-1195..
9. Soken H. S. and hajiyev C., , Reconfigurable UKF for In-Flight Magnetometer Calibration and Attitude Parameter Estimation, 18th IFAC World Congress, Milano-Italy, Vol. 18, No. 1, 2011, pp. 741-746.
10. Shuster D.M., A Survey of Attitude Representations, *Journal of the Astronautically Sciences*, Vol. 41, No. 3, 1993, pp. 439-517
11. Van der Merwe, R., Doucet, A., de Freitas, J. F. G., Wan, E., "The Unscented Particle Filter," *Advances in Neural Information Processing Systems*, 2000, pp. 1-7.
12. Vasconcelos J. F., Elkaim G., Silvestre C., Oliveira P., Cardeira B., "A Geometric Approach to Strap down Magnetometer Calibration in Sensor Frame," *IEEE transactions on Aerospace and Electronic Systems*, Vol. 47, No. 2, 2011, pp. 1293-1306.
13. Wang, K., Li, Y., and Rizos, C., "Practical Approaches to Kalman Filtering with Time-Correlated Measurement Errors," *IEEE Transactions on Aerospace and Electronic Systems*, Vol. 48, No. 2, 2012, pp. 1669-1681.
14. Wu Z., Wu Y., Hu X., Wu M., "Calibration of Three-Axis Strap down Magnetometers Using Particle Swarm Optimization Algorithm," *IEEE International Symposium on Robotic and Sensors Environments (ROSE)*, 2011, pp. 160-165.
15. Zhang, X. and Gao, L., "A Novel Auto-Calibration Method of the Vector Magnetometer," *The 9th International Conference on Electronic Measurement and Instruments*, 2009.
16. Zhang, Z. and Yang, G., "Micro Magnetometer Calibration for Accurate Orientation Estimation," *IEEE Transactions on Biomedical Engineering*, Vol. 99, 2014, pp. 1-8.
17. Zipfel P. H., *Modeling and Simulation of Aerospace Vehicle Dynamics*, edited by J. S. Przemieniecki, *Progress in Astronautics and Aeronautics, AIAA*, New York, 2000, pp. 122-125 and 181-185.